

12. Siegel, M. S. & Isacoff, E. Y. A genetically encoded optical probe of membrane voltage. *Neuron* **19**, 735–741 (1997).
13. Baird, G. S., Zacharias, D. A. & Tsien, R. Y. Circular permutation and receptor insertion within green fluorescent proteins. *Proc. Natl Acad. Sci. USA* **96**, 11241–11246 (1999).
14. Zhang, J., Campbell, R. E., Ting, A. Y. & Tsien, R. Y. Creating new fluorescent probes for cell biology. *Nature Rev. Mol. Cell Biol.* **3**, 906–918 (2002).
15. Sacchetti, A. & Alberli, S. Protein tags enhance GFP folding in eukaryotic cells. *Nature Biotechnol.* **17**, 1046 (1999).
16. Griesbeck, O., Baird, G. S., Campbell, R. E., Zacharias, D. A. & Tsien, R. Y. Reducing the environmental sensitivity of yellow fluorescent protein. *J. Biol. Chem.* **276**, 29188–29194 (2001).
17. Nagai, T. *et al.* A variant of yellow fluorescent protein with fast and efficient maturation for cell-biological applications. *Nature Biotechnol.* **20**, 87–90 (2002).
18. Gross, L. A., Baird, G. S., Hoffman, R. C., Baldrige, K. K. & Tsien, R. Y. The structure of the chromophore within DsRed, a red fluorescent protein from coral. *Proc. Natl Acad. Sci. USA* **97**, 11990–11995 (2000).
19. Bevis, B. J. & Glick, B. S. Rapidly maturing variants of the *Discosoma* red fluorescent protein (DsRed). *Nature Biotechnol.* **20**, 83–87 (2002).
20. Terskikh, A. V., Fradkov, A. F., Zaraisky, A. G., Kajava, A. V. & Angres, B. Analysis of DsRed mutants. Space around the fluorophore accelerates fluorescence development. *J. Biol. Chem.* **277**, 7633–7636 (2002).
21. Terskikh, A. V. *et al.* 'Fluorescent timer': protein that changes color with time. *Science* **290**, 1585–1588 (2000).
22. Duncan, R. R. *et al.* Functional and spatial segregation of secretory vesicle pools according to vesicle age. *Nature* **422**, 176–180 (2003).
23. Patterson, G. H. & Lippincott-Schwartz, J. A photo-activatable GFP for selective photolabeling of proteins and cells. *Science* **297**, 1873–1877 (2002).
24. Ando, R., Hama, H., Yamamoto-Hino, M., Mizuno, H. & Miyawaki, A. An optical marker based on the UV-induced green-to-red photoconversion of a fluorescent protein. *Proc. Natl Acad. Sci. USA* **99**, 12651–12656 (2002).
25. Chudakov, D. M. *et al.* Kindling fluorescent proteins for precise *in vivo* photolabeling. *Nature Biotechnol.* **21**, 191–194 (2003).
26. Campbell, R. E. *et al.* A monomeric red fluorescent protein. *Proc. Natl Acad. Sci. USA* **99**, 7877–7882 (2002).
27. Yanushevich, Y. G. *et al.* A strategy for the generation of non-aggregating mutants of Anthozoa fluorescent proteins. *FEBS Lett.* **511**, 11–14 (2002).
28. Stryer, L. Fluorescence energy transfer as a spectroscopic ruler. *Annu. Rev. Biochem.* **47**, 819–846 (1978).
29. Lakowicz, J. R. in *Principles of Fluorescence Spectroscopy* (ed. Lakowicz, J. R.) 368–391 (Kluwer Academic/Plenum, New York, 1999).
30. Cha, A., Snyder, G. E., Selvin, P. R. & Bezanilla, F. Atomic scale movement of the voltage-sensing region in a potassium channel measured via spectroscopy. *Nature* **402**, 809–813 (1999).
31. Glauner, K. S., Mannuzzi, L. M., Gandhi, C. S. & Isacoff, E. Y. Spectroscopic mapping of voltage sensor movement in the Shaker potassium channel. *Nature* **402**, 813–817 (1999).
32. Ng, T. *et al.* Imaging protein kinase C- $\alpha$  activation in cells. *Science* **183**, 2085–2089 (1999).
33. Verveer, P. J., Wouters, F. S., Reynolds, A. R. & Bastiaens, P. I. H. Quantitative imaging of lateral ErbB1 receptor signal propagation in the plasma membrane. *Science* **290**, 1567–1570 (2000).
34. Kraynov, V. S. *et al.* Localized Rac activation dynamics visualized in living cells. *Science* **290**, 333–337 (2000).
35. Griffin, B. A., Adams, S. R. & Tsien, R. Y. Specific covalent labeling of recombinant protein molecules inside live cells. *Science* **281**, 269–272 (1998).
36. Keppler, A. *et al.* A general method for the covalent labeling of fusion proteins with small molecules *in vivo*. *Nature Biotechnol.* **21**, 86–89 (2003).
37. Griffin, B. A., Adams, S. R. & Tsien, R. Y. Fluorescent labeling of recombinant proteins in living cells with FIAAsH. *Methods Enzymol.* **327**, 565–578 (2000).
38. Gaietta, G. *et al.* Multicolor and electron microscopic imaging of connexin trafficking. *Science* **296**, 503–507 (2002).
39. Falk, M. M. Genetic tags for labeling live cells: gap junctions and beyond. *Trends Cell Biol.* **12**, 399–404 (2002).
40. Marek, K. W. & Davis, G. W. Transgenically encoded protein photoactivation (FIAsh-FAL): acute inactivation of synaptotagmin I. *Neuron* **36**, 805–813 (2002).
41. Farinas, J. & Verkman, A. S. Receptor-mediated targeting of fluorescent probes in living cells. *J. Biol. Chem.* **274**, 7603–7606 (1999).
42. Wu, M. M. *et al.* Mechanisms of pH regulation in the regulated secretory pathway. *J. Biol. Chem.* **276**, 33027–33035 (2001).
43. Chan, W. C. *et al.* Luminescent quantum dots for multiplexed biological detection and imaging. *Curr. Opin. Biotechnol.* **13**, 40–46 (2002).
44. Wu, X. *et al.* Immunofluorescent labeling of cancer marker Her2 and other cellular targets with semiconductor quantum dots. *Nature Biotechnol.* **21**, 41–46 (2003).
45. Jaiswal, J. K., Mattoussi, H., Mauro, J. M. & Simon, S. M. Long-term multiple color imaging of live cells using quantum dot bioconjugates. *Nature Biotechnol.* **21**, 47–51 (2003).
46. Dubertret, B. *et al.* *In vivo* imaging of quantum dots encapsulated in phospholipid micelles. *Science* **298**, 1759–1762 (2002).

## Acknowledgements

We thank Dr Ulrich Nienhaus for providing the spectral data of eqFP611. This work was partly supported by grants from CREST of JST (Japan Science and Technology), and the Japanese Ministry of Education, Science and Technology.

 Online links

## DATABASES

The following terms in this article are linked online to:

LocusLink: <http://www.ncbi.nlm.nih.gov/LocusLink/>  
EGFR | hAGT | PKC- $\alpha$  | PKC- $\gamma$

## FURTHER INFORMATION

Encyclopedia of Life Sciences: <http://www.els.net>  
fluorescence microscopy | fluorescence resonance energy transfer | fluorescence spectrophotometry | fluorescent analogues in biological research

Access to this interactive links box is free online.

## REVIEW

# Photobleaching and photoactivation: following protein dynamics in living cells

Jennifer Lippincott-Schwartz, Nihal Altan-Bonnet and George H. Patterson

Cell biology is being transformed by the use of fluorescent proteins as fusion tags to track protein behaviour in living cells. Here, we discuss the techniques of photobleaching and photoactivation, which can reveal the location and movement of proteins. Widespread applications of these fluorescent-based methods are revealing new aspects of protein dynamics and the biological processes that they regulate.

The discovery and development of fluorescent proteins from marine organisms are revolutionizing the study of cell behaviour by providing convenient markers for gene expression and protein targeting in intact cells and organisms (see also the review on page S1 of this supplement)<sup>1,2</sup>. The most widely used of these fluorescent proteins — green fluorescent protein (GFP) from the jellyfish *Aequorea victoria*<sup>3</sup> — can be attached to virtually any protein of interest and still fold into a fluorescent

molecule. The resulting GFP chimera can be used to localize previously uncharacterized proteins<sup>4</sup> or to visualize and track known proteins to further understand cellular events<sup>5</sup>.

The use of GFP as a minimally invasive tool for studying protein dynamics and function has been stimulated by the engineering of mutant GFPs with improved brightness, photostability and expression properties<sup>2,6,7</sup>. Cells that express proteins tagged with these GFPs can be imaged with low light intensities

over many hours and so can provide useful information about changes in the steady-state distribution of a protein over time. Time-lapse imaging alone, however, cannot reveal a protein's kinetic properties (for example, whether it is freely diffusing, bound to an immobile scaffold, or undergoing binding with and dissociation from other components). Yet, it is these kinetic properties that are arguably of most interest, as they underlie protein function within cells.

In this review, we discuss two techniques — photobleaching and photoactivation — that, when combined with time-lapse imaging, can uncover the kinetic properties of a protein by making its movement observable<sup>2,7–11</sup>. Photobleaching — the photo-induced alteration of a fluorophore that extinguishes its fluorescence — accomplishes this through fluorescence depletion within a selected region. Photoactivation, on the other hand, works by converting molecules to a fluorescent state by using a brief pulse of high-intensity irradiation. After fluorescently highlighting specific populations of molecules by either method, the fluorescent molecules can be followed as they re-equilibrate in the cell. The extent and rate at which this occurs can be quantified and used with computer-modelling approaches to describe the kinetic parameters of a protein.

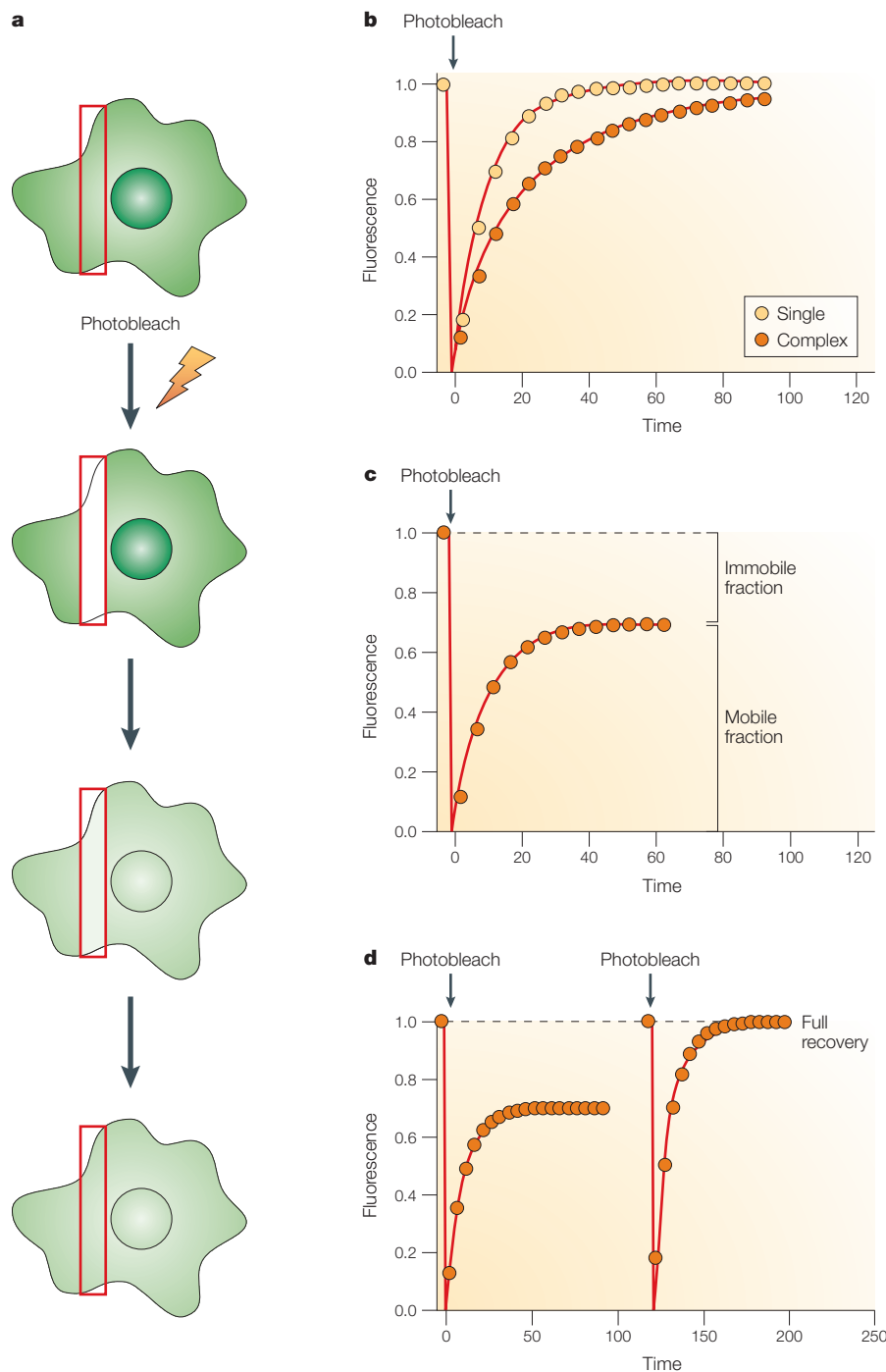


**Figure 1 | Fluorescence recovery after photobleaching.** **a** | A cell expressing fluorescent molecules is imaged with low light levels before and after photobleaching the strip outlined in red. Recovery of fluorescent molecules from the surrounding area into the photobleached region is monitored over time. Analysis usually includes compensation for the reduction in whole-cell fluorescence (depicted in the bottom cartoons). **b** | Fluorescence recovery into the photobleached region can be quantified in a fluorescence recovery after photobleaching (FRAP) curve. These plots depict the recovery for a single species (simulated by a single exponential curve shown in yellow circles) or the kinetics for two equal populations recovering at two different rates (simulated by a double exponential curve shown in orange circles). Note that the kinetics for recovery of the latter takes much longer to plateau. **c** | The level of fluorescence recovery in the photobleached region reveals the mobile and immobile fractions of the fluorophore in the cell (see main text for details). **d** | A simple test for photo-induced immobile fractions is to perform a second FRAP experiment in the same region of interest. In the example here, the mobile fraction of the initial FRAP experiment is ~70%. The level of recovery can be determined by normalizing the fluorescent signal in the region and repeating the FRAP experiment. In the absence of photodamage, full recovery should be observed.

**Photobleaching techniques**

**Fluorescence recovery after photobleaching.** Developed over two decades ago to study the diffusive properties of molecules in living cells<sup>12–17</sup>, fluorescence recovery after photobleaching (FRAP) has experienced a resurgence due to the introduction of GFP and the development of commercially available confocal-microscope-based photobleaching methods<sup>8,11,18</sup>. In this technique, a region of interest is selectively photobleached with a high-intensity laser and the recovery that occurs as molecules move into the bleached region is monitored over time with low-intensity laser light (FIG. 1a). Depending on the protein studied, fluorescence recovery can result from protein diffusion, binding/dissociation or transport processes.

Analysis of fluorescence recovery can be used to determine the kinetic parameters of a protein, including its diffusion constant, mobile fraction, transport rate or binding/dissociation rate from other proteins. In experiments in which the protein of interest moves freely, the fluorescence will recover to the initial prebleach value and the shape of the recovery curve can be described mathematically with a single component recovery (FIG. 1b, single)<sup>19–22</sup>. Determining the effective diffusion coefficient ( $D_{eff}$ ) and mobile fraction ( $M_p$ ) of a protein from such data is relatively straightforward, given the previous analysis of FRAP kinetics<sup>12</sup> (for several recent reviews, see REFS 8,11,18,23). If the shape of the curve is complex (that is, it requires a multi-component diffusion equation<sup>20,24,25</sup>), then multiple populations of the molecule with differing diffusion rates are present (FIG. 1b, complex). This can occur when a molecule undergoes binding and release from intracellular components or exists as a monomer and multimeric forms<sup>10</sup>. Alternatively, the protein might not be diffusing but might be undergoing movement driven by molecular motors or membrane tension flow. A simple test for determining whether a fluorescent protein moves by diffusive movement or facilitated transport is to vary the size of the bleached area or beam radius,  $\omega$ . The recovery will change with an  $\omega^2$  dependence for diffusive movement only<sup>26</sup>. Accurate analysis of FRAP data requires that the bleach event is much shorter than the recovery time and preferably as short as possible. Moreover, the recovery event must be monitored until a recovery plateau is achieved, which is much greater than the half-time for recovery. See TABLE 1 for other FRAP considerations.

**Performing FRAP.** Until recently, carrying out FRAP required custom-built systems to perform the measurements. Development of FRAP methods for use on the laser-scanning confocal microscope has made this technique widely available. Images on the confocal microscope are obtained by scanning a focused laser beam across the specimen and recording the emitted fluorescence through a pinhole that is situated in front of the light detector. One way to photobleach using this system is to define a region-of-interest at the highest possible ZOOM, set the laser power to maximum, and set the laser ATTENUATION to zero. The high zoom increases the dwell time of the laser on the bleached region per line scan (laser intensity increases proportionally to the square of the zoom factor), which therefore greatly increases the radiation per area. But a more advanced method is to use an acousto-optical tunable filter (AOTF; available on more recent commercially available confocal microscopes), which allows rapid (microsecond to millisecond) attenuation of the laser as it scans a field. By allowing rapid switching between the bleaching and normal beam, the AOTF allows accurate measurements of diffusion rates in defined areas.

Use of an AOTF also enables users to photobleach virtually any pattern or shape. This allows FRAP studies to be done on organelles of complex shapes, allowing the lateral mobility of organelle-specific membrane and luminal proteins to be investigated. Selective photobleaching on a confocal microscope also provides a method for analysing aspects of protein dynamics other than diffusion (including assembly/disassembly of protein complexes in cells, the exchange of cytosolic proteins on and off organelles, and the lifetime and fate of membrane-bound transport intermediates<sup>27–30</sup> (FIG. 2a). This type of analysis often requires measuring the fluorescence signal of GFP in a specific structure or area, to compare it with fluorescent intensities of other structures or areas. Once the quantities of fluorescent molecules in different sites or states are known, computer modelling can then be used to determine the parameter values (that is, the rate constants for binding interactions and exchange times) of the processes of interest<sup>10</sup>. Recent applications in which kinetic modelling has been used successfully include analysing the dynamics of nuclear proteins<sup>31–35</sup>, protein transport through membrane trafficking pathways<sup>27,36,37</sup> and membrane coat protein dynamics<sup>30</sup>.

**Inverse FRAP.** Inverse FRAP (iFRAP) is performed as a normal FRAP experiment with the exception that the molecules outside a

Table 1 | **FRAP considerations**

Problem	Potential explanations	References
Lack of recovery or partial recovery after photobleach	Possible explanations include: an immobile fraction of unbleached molecules in the cytoplasm that could not diffuse into the bleached region; an immobile fraction of molecules in the bleached area that was unable to exchange with the incoming unbleached molecules; or the bleached area is not continuous with the rest of the cell (for example, a separate membrane compartment).	8
Reversible photobleaching of GFP	The excitation might cause the GFP molecule to flicker or to be sequestered in a triplet state. Both of these situations can result in the recovery of fluorescence (in milliseconds to several seconds) of the GFP molecule in the absence of diffusion. To control for any reversible photobleaching of the GFP in a FRAP experiment, the FRAP conditions should be repeated in fixed samples in which no recovery of fluorescence should be expected. Or, alternatively, the bleach spot size could be varied and the changes in the timescale of recovery could be confirmed.	86
Non-diffusive behaviour	Measurements in FRAP studies are often complicated by the binding and dissociation of fluorescent molecules to and from intracellular components. This is usually reflected in the FRAP curves by longer recovery times, by an incomplete recovery (an immobile fraction) or by the presence of several slopes (indicating several recovery processes over different timescales). Kinetic modelling methods, along with computer simulations, have been useful tools to dissect and analyse the recovery curves obtained by FRAP. A kinetic model is characterized by biophysical parameters, such as binding and release rate constants, diffusion constants, flow rates and residence times. The model can be simulated on the computer for different parameter values. Once the parameters that best fit the experimental data have been determined, the predictions of the model can be tested experimentally.	10,30
D values of the same ROI in the same cell in two consecutive experiments are different	A potential explanation is damage to the photobleached area. Decreasing the bleach time, acquisition time or the excitation beam intensity during the recovery period could avoid damaging the cell. Using YFP rather than GFP or CFP will also make it easier to photobleach.	87

CFP, cyan fluorescent protein; FRAP, fluorescence recovery after photobleaching; GFP, green fluorescent protein; ROI, region of interest; YFP, yellow fluorescent protein.

region of interest are photobleached and the loss of fluorescence from the non-photobleached region is monitored over time. As opposed to the rate of recovery studied using a FRAP experiment, iFRAP offers a way to monitor the rate of movement out of a region. For example, iFRAP was used to monitor the dissociation kinetics of GFP-tagged RNA polymerase I components from sites of rRNA transcription<sup>34</sup>. Because this method indirectly highlights a pool of molecules by decreasing the background fluorescence, it has also been used to follow Golgi to plasma membrane transport carriers as they moved from the Golgi and fused with the plasma membrane<sup>27,37</sup> (FIG. 2c).

#### **Fluorescence localization after photobleaching.**

Fluorescence localization after photobleaching (FLAP)<sup>38</sup> also indirectly highlights a pool of molecules. For a FLAP experiment, the same protein-of-interest is tagged with two different fluorophores that co-localize when expressed in cells. By photobleaching one of these fluorophores, a selected pool can be

highlighted and followed over time. Using cyan fluorescent protein (CFP)- and yellow fluorescent protein (YFP)-tagged  $\beta$ -actin, monomer versus filamentous actin dynamics was demonstrated<sup>38</sup>, and actin transport was monitored during cell protrusion<sup>39</sup>. In another study, CFP- and YFP-tagged histone H2B molecules were co-expressed in cells undergoing mitosis<sup>40</sup>. After one pool of the YFP-containing H2B molecules was photobleached, the movement of the non-photobleached pool was used to monitor chromosome positions throughout the cell cycle.

**Fluorescence loss in photobleaching.** Complementary to the photobleaching techniques discussed earlier, the continuity of a cell compartment can be monitored using a technique called fluorescence loss in photobleaching (FLIP) (FIG. 2b). In a FLIP experiment, a fluorescent cell is repeatedly photobleached within a small region while the whole cell is repeatedly imaged. Any regions of the cell that are connected to the area being bleached will gradually lose fluorescence due to lateral



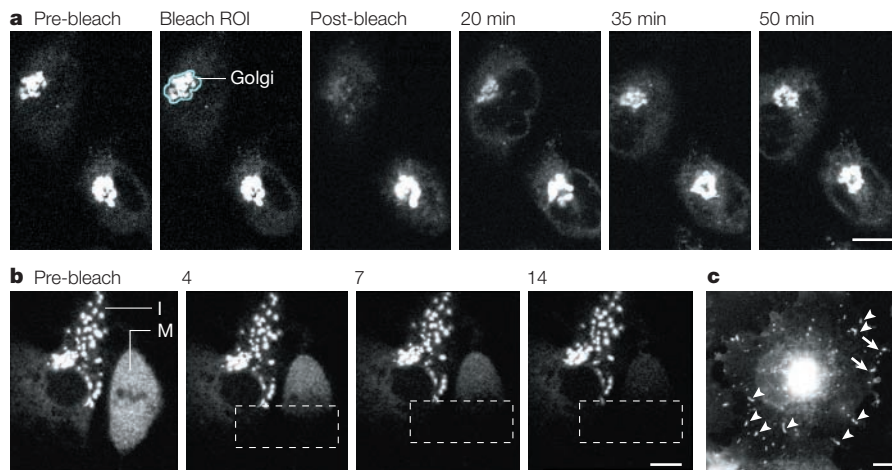


**Figure 2 | Photobleaching of GFP-tagged proteins to monitor dynamics.** **a** | The Golgi complex (blue outline) was photobleached in a cell expressing galactase-GFP (green fluorescent protein) in the presence of cycloheximide and the recovery was monitored over time (post-bleach image = time 0). The observed recovery indicated galactase-GFP resident in the Golgi undergoes continuous exchange with non-Golgi pools (such as those in the endoplasmic reticulum) during its lifetime. **b** | Fluorescence loss in photobleaching (FLIP) of galactase-GFP in interphase and mitotic cells. A boxed area spanning an interphase and a metaphase cell was repetitively photobleached with high-intensity laser light over time. After each photobleach, an image of the entire field was scanned with low-intensity laser light. The number of bleach cycles is indicated in each panel. Note that in a metaphase cell, unlike in interphase, the galactase-GFP fluorescence is rapidly lost after 14 cycles of photobleaching (see [Movie 1](#) online). This indicates that it is in a continuous compartment in which it can rapidly diffuse. Images in **b** are reproduced from REF. 36 © (1999) Elsevier Science. **c** | Dimly fluorescent structures can be visualized using inverse fluorescence recovery after photobleaching (iFRAP). The transport of vesicular stomatitis virus G protein (VSV-G-GFP) in membrane-bound carriers from the Golgi to the plasma membrane was visualized by photobleaching a region of interest, which included the whole cell except the Golgi complex. After the photobleach, the export of GFP-tagged VSV-G-GFP from the Golgi complex could be imaged with low laser light (arrows) (see [Movie 2](#) online). The images in **a** and **c** are reproduced with permission from Lippincott-Schwartz, J. et al. *Histochem. Cell Biol.* 116, 97–107 © (2001) Springer-Verlag.

movement of mobile proteins into this area. By contrast, the fluorescence in unconnected regions will not be affected. In addition to assessing continuity between areas of the cell, FLIP can be used to assess whether a protein moves uniformly across a particular cell compartment or undergoes interactions that impede its motion<sup>28,36,41</sup>. Furthermore, it can be used to reveal faint fluorescence in unconnected compartments that normally cannot be seen against the bright fluorescence that arises in other parts of the cell<sup>42</sup>.

#### Photobleaching applications

Photobleaching techniques that are applied to live-cell imaging are transforming our understanding of cellular organization and dynamics. For the first time, the mobility of diverse molecules in the cytoplasm, nucleus, organelle lumens and membranes of living cells can be measured, and the viscosity of these environments analysed. Moreover, resident components of organelles, once thought to be stable, have been shown to continuously enter and exit these structures. These findings are defining the biophysical characteristics of

cellular compartments and their components, and are illuminating regulatory features of signalling and transport pathways.

**Protein dynamics in the cytoplasm.** The cytoplasm contains numerous macromolecular assemblies and cytoskeletal elements (including microtubules, actin and intermediate filaments). Yet, it has only recently become clear from FRAP studies that small molecules can rapidly diffuse through this system and bind reversibly to dynamic scaffolds. Such studies have shown that molecules up to 200 kDa undergo unhindered diffusion through the cytoplasm with  $D_{eff}$  values several times lower than those found in water<sup>43,44</sup>. By contrast, larger molecules (>200 kDa) or macromolecular complexes have impeded diffusion, presumably due to the extensive cytoskeletal meshwork of cells<sup>44–46</sup>.

These diffusional properties have recently been shown to participate in the spatial organization and activity of signalling pathways. One example is the mitogen-activated protein kinase (MAPK) pathway. FRAP studies<sup>47</sup> that examined the dynamics of the MAPK **Fus3** in

yeast showed that it continuously binds to and dissociates from a plasma-membrane-localized scaffold molecule, **Ste5**. After being activated at the plasma membrane when bound to **Ste5**, **Fus3** rapidly relocates to the nucleus by diffusion. The spatial localization of **Fus3** activation and its dynamics at the plasma membrane are thought to help control and amplify MAPK signalling. A second example from yeast is the behaviour of septins — small GTPases that recruit proteins to form a ring at the cleavage site during cell division. Using FRAP, GFP-tagged septins in yeast were shown to be mobile during most of the cell cycle but then to become immobilized at the cleavage site at the time of budding<sup>48</sup>. This leads to the recruitment of other proteins to this site, and thereby creates a diffusion barrier between mother and daughter cells<sup>49</sup>. So, by changing between mobile and immobile states, septins help to control the temporal and spatial regulation of cytokinesis.

**Protein dynamics in the nucleus.** FRAP measurements of GFP-labelled nuclear proteins have revealed that many compartments in the nucleus — including nucleoli, Cajal bodies and splicing-factor compartments — are not stable entities but are steady-state assemblies of proteins that undergo continuous association and dissociation<sup>31–35</sup>. The diffusion of proteins (including **HMG17**, **SF2/ASF**, fibrillarin, coilin and **TBP**) and the U7 small nuclear RNA (snRNA) in these subnuclear compartments are significantly lower ( $D_{eff}$  between 0.24–0.53  $\mu\text{m}^2 \text{sec}^{-1}$ ) than reported for freely diffusing peptides, GFP molecules or fluorescently labelled dextrans ( $\geq 2 \mu\text{m}^2 \text{sec}^{-1}$ )<sup>46,50</sup>. This indicates that exchange into and out of subnuclear compartments is the rate-limiting factor for the movement of these proteins and snRNA within the nucleus. In addition to providing insights into the dynamics of subnuclear structures, FRAP studies of the nucleus have revealed the kinetics of the binding of transcription-factor machinery to DNA promoters<sup>51,52</sup>, the intranuclear mobility of messenger RNA<sup>53</sup> and the geography of chromosomes<sup>40,54</sup>.

**Intra- and inter-organelle dynamics.** The micro-environment within organelles and the exchange of components between organelles have also been probed using FRAP. One example is the mitochondrial matrix, which has traditionally been thought of as too dense to allow the rapid movement of its components. However, FRAP measurements of the GFP-tagged matrix enzyme cytochrome oxidase *c* revealed that this small enzyme diffuses extremely rapidly in mitochondria<sup>55</sup>.

By contrast, components of the large macromolecular assemblies that comprise the fatty acid  $\beta$ -oxidation pathway were immobilized, presumably through associations with the inner mitochondrial membrane<sup>56</sup>. Based on these findings, it is thought that the clustered assemblies of proteins that are immobilized in the mitochondrial matrix provide a surface on which highly mobile substrates and enzymes can interact<sup>55,56</sup>.

FRAP has also unveiled important characteristics of the ER lumen, which is enriched in molecules that are involved in protein biogenesis, folding and assembly. Under normal conditions, small soluble proteins can diffuse rapidly throughout the ER lumen with access to all areas<sup>42,57</sup>. However, under conditions of cell stress — such as heat shock, change in osmolarity, calcium depletion, a glycosylation block or the production of unfolded proteins<sup>42,58–60</sup> — there are marked changes in the mobility of proteins and luminal continuity. So, the ER lumen is not a stable environment, but undergoes significant global changes in response to cell stress, which could affect its numerous cellular roles.

FRAP techniques have been crucial for characterizing the mobility of GFP-tagged proteins that are embedded in organelle bilayers. The measured  $D_{eff}$  for many transmembrane proteins localized in the ER, Golgi apparatus or plasma membrane have values ranging from 0.2 to 0.5  $\mu\text{m}^2 \text{sec}^{-1}$  with little or no immobile fractions<sup>41,42,61</sup>. This indicates that these proteins have unhindered lateral mobility in the membranes of these compartments. By contrast, large assemblies of membrane proteins in the ER (for example, translocons, TAP transporters and nuclear pores) or plasma-membrane proteins interacting with the extracellular matrix or cortical cytoskeletal elements, diffuse more slowly or have large immobile fractions<sup>25,60,62–65</sup>. Studies of the diffusion properties of these molecules have important implications for understanding how proteins are retained in different membrane-bound compartments, and what mechanisms coordinate the processing and transport functions of membranes. For instance, alterations in TAP1–GFP  $D_{eff}$  under different peptide loads have provided evidence of TAP-complex conformational changes and interactions with class I major histocompatibility complex (MHC) molecules during peptide translocation<sup>25,66</sup>. Additionally, FRAP experiments performed on the **lamin-B receptor** at various points during the cell cycle show that although the receptor is immobile in the nuclear envelope during interphase, it disperses to the endoplasmic reticulum (ER) and is completely mobile during mitosis<sup>67</sup>.

Organelles of the secretory pathway, including the Golgi apparatus, have traditionally been thought to contain relatively stable resident components. But recent studies using FRAP techniques have revealed that membrane-bound and peripherally associated Golgi-resident proteins associate only transiently with this organelle<sup>68</sup>. Whereas transmembrane enzymes can reside in the Golgi for up to 1–2 hours before recycling to the ER, peripherally associated coat and matrix proteins on the Golgi exchange with the soluble pools in the cytoplasm every 30–60 seconds. These results indicate that the Golgi apparatus is a highly dynamic organelle, the

identity of which depends on continuous protein exchange with the cytoplasm and ongoing membrane input/output pathways.

Finally, photobleaching techniques have provided a powerful method for highlighting transport intermediates as they move along specific membrane-trafficking pathways<sup>27,37,69,70</sup> (FIG. 2b) and for analysing the dynamics of the protein-trafficking machinery<sup>29,30,40,71</sup>. Studies of GFP-tagged components of membrane-trafficking machinery that sorts cargo into membrane-bound transport intermediates have shown that they undergo continuous binding to and dissociation from membranes irrespective of vesicle budding.

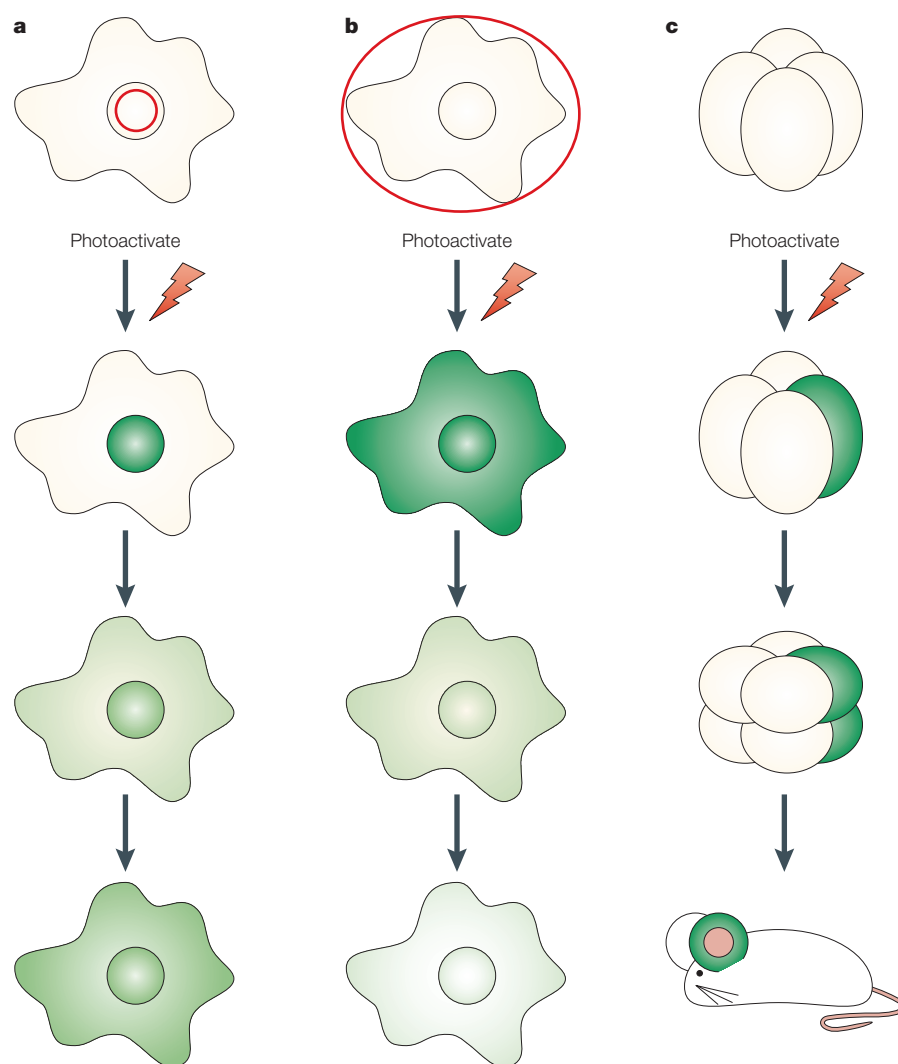


**Figure 3 | Photoactivation of fluorescent proteins. a** | Before photoactivation, cells expressing photoactivatable proteins display little fluorescence in the spectral region that is used for detecting enhanced fluorescence. After photoactivation of a selected region (indicated in red), an increase in fluorescence is observed. By directly highlighting specific populations of molecules, such as the nuclear pool of the fluorophore, the movement from this region throughout the cell can be monitored. **b** | Alternatively, the entire cell can be photoactivated and the fate of the fluorescence followed over time. Because newly synthesized proteins are not detected nor photoactivated during the imaging experiment, photoactivatable fluorescent proteins circumvent this possible artefact and might allow the fate of fluorescently tagged proteins to be monitored by ‘optical pulse labelling’. **c** | Photoactivation of a single cell or population of cells can be used to monitor cell lineage within a developing organism.

## REVIEWS

These include COPII (*Sec23/Sec24* and *Sec13/31* heterodimers assembled onto ER membranes with the small GTPase, *Sar1*), COPI (a heptameric cytosolic protein complex recruited to Golgi membranes), *Arf1* (a small GTPase) and clathrin (a major structural constituent forming the lattice around clathrin-coated vesicles). Whether this exchange represents a 'proof-reading' mechanism for ensuring proper loading of coated vesicles, or is necessary for lateral membrane differentiation into pleiomorphic transport intermediates<sup>72</sup>, remains to be investigated. In either case, the kinetics of this exchange have major implications for models of coat protein function and of the GTP binding and hydrolysis cycles of *Arf1* and *Sar1*.

### Photoactivation

Photoactivation is the photo-induced activation of an inert molecule to an active state. It is generally associated with the ultraviolet-light-induced release of a caging group from a 'caged' compound. Photoactivation of CAGED COMPOUNDS in the study of living cells is reviewed elsewhere<sup>73</sup>, so our discussion is limited to recent advances in the development of genetically encoded photoactivatable fluorescent proteins.

Included in the development and discovery of new fluorescent protein variants<sup>2,6,7</sup> (see also the review on page S1 of this supplement) were attempts to produce photoactivatable fluorescent proteins. These studies yielded several molecules or techniques for optically highlighting proteins, but each had drawbacks for use in living cells, such as modest activation<sup>74,75</sup>, low stability<sup>76</sup> or a requirement for low oxygen conditions<sup>77,78</sup>. Recently, three photoactivatable fluorescent proteins — photoactivatable GFP (PA-GFP)<sup>79</sup>, Kaede<sup>80</sup> and kindling fluorescent protein 1 (KFP1)<sup>81</sup> — have been reported that offer improvements over the earlier versions.

The PA-GFP<sup>79</sup> was developed with the aim of optimizing the photoconversion properties of *Aequorea victoria* wtGFP<sup>74</sup>, which produces only a ~threefold increase in fluorescence under 488 nm excitation. Mutation of threonine 203 to histidine in wtGFP to produce PA-GFP decreases the initial absorbance in the minor peak region (~475 nm) and leads to ~100-fold increase after photoactivation<sup>79</sup>. Alternatively, for the Kaede protein, isolated from *Trachyphyllia geoffroyi*, photoactivation results in a 2,000-fold increase in its red-to-green fluorescence ratio<sup>80</sup>. Finally, KFP1 — an A148G mutant (where A is alanine and G is glycine) of asFP595 (asCP, where 'FP' is fluorescent protein and 'CP' is chromoprotein) from the sea anemone,

*Anemonia sulcata* — gives a 30-fold increase in red fluorescence after photoactivation<sup>81</sup>.

All of these molecules share the common characteristic of displaying low levels of fluorescence before photoactivation and higher levels after photoactivation. In a typical experiment, a cell or organism that is expressing the photoactivatable fluorescent protein is imaged at one wavelength prior to, and at various intervals after, photoactivation of a selected region with a different wavelength. However, the properties of each protein, including the wavelengths used for imaging and photoactivation, offer distinct advantages and disadvantages. For example, PA-GFP and Kaede both require ~400 nm light for photoactivation, whereas KFP1 uses green light (532 nm), which is probably better for use with living cells. Kaede displays a remarkable 2,000-fold increase in its red-to-green fluorescence ratio, but the use of both the red and green fluorescence bands could make multilabel experiments problematic. On the other hand, the green fluorescence of Kaede is bright enough to visualize the localization of the non-photoactivated proteins easily, whereas visualizing PA-GFP and KFP1 is more problematic due to their low fluorescence before photoactivation. The self-association properties of Kaede and KFP1 into tetrameric forms limit their usefulness as protein fusion tags because tetramerization might perturb parent protein localization and trafficking. The recent engineering of the *DsRed* protein into a monomeric form<sup>82</sup> is encouraging for the possibility of the eventual disruption of Kaede and KFP1 into monomers. Variants that are derived from *A. victoria*, such as PA-GFP, self-associate to a lesser degree, and even those interactions can be disrupted by one of three further point mutations<sup>83</sup>. Because of this, PA-GFP can be used as a reliable tag for creating fluorescent reporter molecules.

The ability to 'switch on' the fluorescence of the photoactivatable proteins makes them excellent tools for exploring protein behaviour in living cells. As the fluorescence of these proteins comes only after photoactivation, newly synthesized non-photoactivated pools are unobserved and do not complicate experimental results (FIG. 3a). This signal independence from new protein synthesis could allow the study of protein degradation of tagged molecules by 'optical pulse labelling' and monitoring of the fluorescence over time (FIG. 3b). Photoactivation of these proteins is generally rapid and gives stable fluorescence signals. Therefore, they can be used to examine various kinetic properties of tagged proteins, such as their  $D_{\text{eff}}$ ,  $M_p$ , compartmental residency time and exchange. Lastly, cell

lineage or movement in a developing organism can be monitored by imaging the fluorescence dispersion after photoactivation of a single cell or subpopulation of cells<sup>81</sup> (FIG. 3c). So, these proteins have remarkable promise to complement and extend the range of present fluorescent-protein imaging applications.

### Concluding remarks

The battery of fluorescent proteins and imaging tools that allow us to monitor protein dynamics in living cells continue to provide numerous new insights into the behaviour of proteins, organelles and cells. In so doing, they have ushered in a new era of cell biology in which kinetic microscopy methods can be used to decipher pathways and mechanisms of biological processes. The microscopy techniques of photobleaching and photoactivation are perhaps the most versatile and widely used of these methods. Their ability to alter the fluorescence steady state without perturbing protein dynamics offers unprecedented opportunities for obtaining quantitative information about protein concentrations, diffusion rates, binding kinetics and protein lifetimes in single live cells, which have been indiscernible using traditional biochemical approaches. Such information is paramount to understanding how biological processes unfold, are regulated and interact in the living cell.

Looking to the future, photobleaching and photoactivation will almost certainly continue to provide important new results as their applications are extended by the development of newer instruments that push the limits of temporal and spatial detection, and by the discovery of brighter and differently coloured fluorescent proteins. For example, FRAP can be combined with other microscopic imaging approaches, including two-photon microscopy<sup>84</sup>, (see MULTI-PHOTON MICROSCOPY) or TOTAL INTERNAL REFLECTION MICROSCOPY<sup>85</sup>, to study events at specific sites in the cell. And, photobleaching or photoactivation can be combined with fluorescence energy-transfer techniques<sup>2,8</sup> to study protein interactions with greater precision. These advances will continue to require computational approaches to comprehend the plethora of quantitative experimental data<sup>10</sup>, as well as new database tools for the analysis of specific models and their relationship to other more complex models.

*Cell Biology and Metabolism Branch,  
National Institute of Child Health and Human  
Development, Building 18T/Room 101, National  
Institutes of Health, Bethesda, Maryland 20892, USA.  
Correspondence to J.L.-S.  
e-mail: jlippin@helix.nih.gov*

*Please cite this article as a supplement to volume 5  
of Nature Cell Biology, pages S7–S14.  
doi:10.1038/ncb1032*



1. van Roessel, P. & Brand, A. H. Imaging into the future: visualizing gene expression and protein interactions with fluorescent proteins. *Nature Cell Biol.* **4**, E15–E20 (2002).
2. Zhang, J., Campbell, R. E., Ting, A. Y. & Tsien, R. Y. Creating new fluorescent probes for cell biology. *Nature Rev. Mol. Cell Biol.* **3**, 906–918 (2002).
3. Chalfie, M., Tu, Y., Euskirchen, G., Ward, W. W. & Prasher, D. C. Green fluorescent protein as a marker for gene expression. *Science* **263**, 802–805 (1994).
4. González, C. & Bejarano, L. A. Protein traps: using intracellular localization for cloning. *Trends Cell Biol.* **10**, 162–165 (2000).
5. Lippincott-Schwartz, J., Roberts, T. H. & Hirschberg, K. Secretory protein trafficking and organelle dynamics in living cells. *Annu. Rev. Cell Dev. Biol.* **16**, 557–589 (2000).
6. Tsien, R. Y. The green fluorescent protein. *Annu. Rev. Biochem.* **67**, 509–544 (1998).
7. Lippincott-Schwartz, J. & Patterson, G. H. Development and use of fluorescent protein markers in living cells. *Science* **300**, 87–91 (2003).
8. Lippincott-Schwartz, J., Snapp, E. & Kenworthy, A. Studying protein dynamics in living cells. *Nature Rev. Mol. Cell Biol.* **2**, 444–456 (2001).
9. Houtsmuller, A. B. & Vermeulen, W. Macromolecular dynamics in living cell nuclei revealed by fluorescence redistribution after photobleaching. *Histochem. Cell Biol.* **115**, 13–21 (2001).
10. Phair, R. D. & Misteli, T. Kinetic modeling approaches to *in vivo* imaging. *Nature Rev. Mol. Cell Biol.* **2**, 898–907 (2001).
11. Klonis, N. *et al.* Fluorescence photobleaching analysis for the study of cellular dynamics. *Eur. Biophys. J.* **31**, 36–51 (2002).
12. Axelrod, D., Koppel, D. E., Schlessinger, J., Elson, E. & Webb, W. W. Mobility measurement by analysis of fluorescence photobleaching recovery kinetics. *Biophys. J.* **16**, 1055–1069 (1976).
13. Elson, E. L., Schlessinger, J., Koppel, D. E., Axelrod, D. & Webb, W. W. Measurement of lateral transport on cell surfaces. *Prog. Clin. Biol. Res.* **9**, 137–147 (1976).
14. Jacobson, K., Derzko, Z., Wu, E. S., Hou, Y. & Poste, G. Measurement of the lateral mobility of cell surface components in single, living cells by fluorescence recovery after photobleaching. *J. Supramol. Struct.* **5**, 565(417)–576(428) (1976).
15. Schlessinger, J. *et al.* Lateral transport on cell membranes: mobility of concanavalin A receptors on myoblasts. *Proc. Natl Acad. Sci. USA* **73**, 2409–2013 (1976).
16. Schindler, M., Osborn, M. J. & Koppel, D. E. Lateral diffusion of lipopolysaccharide in the outer membrane of *Salmonella typhimurium*. *Nature* **285**, 261–263 (1980).
17. Sheetz, M. P., Schindler, M. & Koppel, D. E. Lateral mobility of integral membrane proteins is increased in spherocytic erythrocytes. *Nature* **285**, 510–511 (1980).
18. Reits, E. A. J. & Neefjes, J. J. From fixed to FRAP: measuring protein mobility and activity in living cells. *Nature Cell Biol.* **3**, E145–E147 (2001).
19. Kao, H. P., Abney, J. R. & Verkman, A. S. Determinants of the translational mobility of a small solute in cell cytoplasm. *J. Cell Biol.* **120**, 175–184 (1993).
20. Gordon, G. W., Chazotte, B., Wang, X. F. & Herman, B. Analysis of simulated and experimental fluorescence recovery after photobleaching. Data for two diffusing components. *Biophys. J.* **68**, 766–778 (1995).
21. Verkman, A. S. Solute and macromolecule diffusion in cellular aqueous compartments. *Trends Biochem. Sci.* **2**, 27–33 (2002).
22. Siggia, E. D., Lippincott-Schwartz, J. & Bekiranov, S. Diffusion in inhomogeneous media: theory and simulations applied to whole cell photobleach recovery. *Biophys. J.* **79**, 1761–1770 (2000).
23. Snapp, E. L., Altan, N. & Lippincott-Schwartz, J. in *Current Protocols in Cell Biology* (eds Bonifacino, J., Dasso, M., Harford, J. B., Lippincott-Schwartz, J. & Yamada, K. M.) 21.1.1–21.1.23 (John Wiley & Sons, Inc., New York, 2003).
24. Periasamy, N. & Verkman, A. S. Analysis of fluorophore diffusion by continuous distributions of diffusion coefficients: application to photobleaching measurements of multicomponent and anomalous diffusion. *Biophys. J.* **75**, 557–567 (1998).
25. Marguet, D. *et al.* Lateral diffusion of GFP-tagged H2Ld molecules and of GFP-TAP1 reports on the assembly and retention of these molecules in the endoplasmic reticulum. *Immunity* **11**, 231–240 (1999).
26. Wu, E. S., Jacobson, K., Szoka, F. & Portis, J. A. Lateral diffusion of a hydrophobic peptide, N-4-nitrobenz-2-oxa-1,3-diazole gramicidin S, in phospholipid multibilayers. *Biochemistry* **17**, 5543–5550 (1978).
27. Hirschberg, K. *et al.* Kinetic analysis of secretory protein traffic and characterization of Golgi to plasma membrane transport intermediates in living cells. *J. Cell Biol.* **143**, 1485–1503 (1998).
28. Phair, R. D. & Misteli, T. High mobility of proteins in the mammalian nucleus. *Nature* **404**, 604–609 (2000).
29. Wu, X. *et al.* Clathrin exchange during clathrin-mediated endocytosis. *J. Cell Biol.* **155**, 291–300 (2001).
30. Presley, J. F. *et al.* Dissection of COPI and Arf1 dynamics *in vivo* and role in Golgi membrane transport. *Nature* **417**, 187–193 (2002).
31. Misteli, T., Cáceres, J. F. & Spector, D. L. The dynamics of a pre-mRNA splicing factor in living cells. *Nature* **387**, 523–527 (1997).
32. Snaar, S., Wiesmeijer, K., Jochemsen, A. G., Tanke, H. J. & Dirks, R. W. Mutational analysis of fibrillarin and its mobility in living human cells. *J. Cell Biol.* **151**, 653–662 (2000).
33. Chen, D., Hinkley, C. S., Henry, R. W. & Huang, S. TBP dynamics in living human cells: constitutive association of TBP with mitotic chromosomes. *Mol. Biol. Cell* **13**, 276–284 (2002).
34. Dundr, M. *et al.* A kinetic framework for a mammalian RNA polymerase *in vivo*. *Science* **298**, 1623–1626 (2002).
35. Handwerker, K. E., Murphy, C. & Gall, J. G. Steady-state dynamics of Cajal body components in the *Xenopus* germinal vesicle. *J. Cell Biol.* **160**, 495–504 (2003).
36. Zaal, K. J. M. *et al.* Golgi membranes are absorbed into and reemerge from the ER during mitosis. *Cell* **99**, 589–601 (1999).
37. Nichols, B. J. *et al.* Rapid cycling of lipid raft markers between the cell surface and Golgi complex. *J. Cell Biol.* **153**, 529–541 (2001).
38. Dunn, G. A., Dobbie, I. M., Monypenny, J., Holt, M. R. & Zicha, D. Fluorescence localization after photobleaching (FLAP): a new method for studying protein dynamics in living cells. *J. Microsc.* **205**, 109–112 (2002).
39. Zicha, D. *et al.* Rapid actin transport during cell protrusion. *Science* **300**, 142–145 (2003).
40. Gerlich, D. *et al.* Global chromosome positions are transmitted through mitosis in mammalian cells. *Cell* **112**, 751–764 (2003).
41. Cole, N. B. *et al.* Diffusional mobility of Golgi proteins in membranes of living cells. *Science* **273**, 797–801 (1996).
42. Nehls, S. *et al.* Dynamics and retention of misfolded proteins in native ER membranes. *Nature Cell Biol.* **2**, 288–295 (2000).
43. Luby-Phelps, K., Taylor, D. L. & Lanni, F. Probing the structure of cytoplasm. *J. Cell Biol.* **102**, 2015–2022 (1986).
44. Swaminathan, R., Hoang, C. P. & Verkman, A. S. Photobleaching recovery and anisotropy decay of green fluorescent protein GFP-S65T in solution and cells: cytoplasmic viscosity probed by green fluorescent protein translational and rotational diffusion. *Biophys. J.* **72**, 1900–1907 (1997).
45. Luby-Phelps, K., Castle, P. E., Taylor, D. L. & Lanni, F. Hindered diffusion of inert tracer particles in the cytoplasm of mouse 3T3 cells. *Proc. Natl Acad. Sci. USA* **84**, 4910–4913 (1987).
46. Seksek, O., Biwersi, J. & Verkman, A. S. Translational diffusion of macromolecule-sized solutes in cytoplasm and nucleus. *J. Cell Biol.* **138**, 131–142 (1997).
47. van Drogen, F., Stucke, V. M., Jorritsma, G. & Peter, M. MAP kinase dynamics in response to pheromones in budding yeast. *Nature Cell Biol.* **3**, 1051–1059 (2001).
48. Dobbelaere, J., Gentry, M. S., Hallberg, R. L. & Barral, Y. Phosphorylation-dependent regulation of septin dynamics during the cell cycle. *Dev. Cell* **4**, 345–357 (2003).
49. Faty, M., Fink, M. & Barral, Y. Septins: a ring to part mother and daughter. *Curr. Genet.* **41**, 123–131 (2002).
50. Reits, E. *et al.* Peptide diffusion, protection, and degradation in nuclear and cytoplasmic compartments before antigen presentation by MHC Class I. *Immunity* **18**, 97–108 (2003).
51. Becker, M. *et al.* Dynamic behavior of transcription factors on a natural promoter in living cells. *EMBO Rep.* **3**, 1188–1194 (2002).
52. Kimura, H., Sugaya, K. & Cook, P. R. The transcription cycle of RNA polymerase II in living cells. *J. Cell Biol.* **159**, 777–782 (2002).
53. Calapez, A. *et al.* The intranuclear mobility of messenger RNA binding proteins is ATP dependent and temperature sensitive. *J. Cell Biol.* **159**, 795–805 (2002).
54. Walter, J., Schermelleh, L., Cremer, M., Tashiro, S. & Cremer, T. Chromosome order in HeLa cells changes during mitosis and early G1, but is stably maintained during subsequent interphase stages. *J. Cell Biol.* **160**, 685–697 (2003).
55. Partikian, A., Ölvéczky, B., Swaminathan, R., Li, Y. & Verkman, A. S. Rapid diffusion of green fluorescent protein in the mitochondrial matrix. *J. Cell Biol.* **140**, 821–829 (1998).
56. Haggie, P. M. & Verkman, A. S. Diffusion of tricarboxylic acid cycle enzymes in the mitochondrial matrix *in vivo*. Evidence for restricted mobility of a multienzyme complex. *J. Biol. Chem.* **277**, 40782–40788 (2002).
57. Dayel, M. J., Horn, E. F. Y. & Verkman, A. S. Diffusion of green fluorescent protein in the aqueous-phase lumen of endoplasmic reticulum. *Biophys. J.* **76**, 2843–2851 (1999).
58. Subramanian, K. & Meyer, T. Calcium-induced restructuring of nuclear envelope and endoplasmic reticulum calcium stores. *Cell* **89**, 963–971 (1997).
59. Terasaki, M. Dynamics of the endoplasmic reticulum and Golgi apparatus during early sea urchin development. *Mol. Biol. Cell* **11**, 897–914 (2000).
60. Nikonov, A. V., Snapp, E. L., Lippincott-Schwartz, J. & Kreibich, G. Active translocon complexes labeled with GFP-Dad1 diffuse slowly as large polysome arrays in the endoplasmic reticulum. *J. Cell Biol.* **158**, 497–506 (2002).
61. Schmoranzler, J., Goulian, M., Axelrod, D. & Simon, S. M. Imaging constitutive exocytosis with total internal reflection fluorescence microscopy. *J. Cell Biol.* **149**, 23–32 (2000).
62. Barbour, S. & Edidin, M. Cell-specific constraints to the lateral diffusion of a membrane glycoprotein. *J. Cell Physiol.* **150**, 526–533 (1992).
63. Chakrabarti, A., Matko, J., Rahman, N. A., Barisas, B. G. & Edidin, M. Self-association of class I major histocompatibility complex molecules in liposome and cell surface membranes. *Biochemistry* **31**, 7182–7189 (1992).
64. Daigle, N. *et al.* Nuclear pore complexes form immobile networks and have a very low turnover in live mammalian cells. *J. Cell Biol.* **154**, 71–84 (2001).
65. Griffis, E. R., Altan, N., Lippincott-Schwartz, J. & Powers, M. A. Nup98 is a mobile nucleoporin with transcription-dependent dynamics. *Mol. Cell Biol.* **13**, 1282–1297 (2002).
66. Reits, E. A. J., Vos, J. C., Grommé, M. & Neefjes, J. The major substrates for TAP *in vivo* are derived from newly synthesized proteins. *Nature* **404**, 774–778 (2000).
67. Ellenberg, J. *et al.* Nuclear membrane dynamics and reassembly in living cells: targeting of an inner nuclear membrane protein in interphase and mitosis. *J. Cell Biol.* **138**, 1193–1206 (1997).
68. Ward, T. H., Polishchuk, R. S., Caplan, S., Hirschberg, K. & Lippincott-Schwartz, J. Maintenance of Golgi structure and function depends on the integrity of ER export. *J. Cell Biol.* **155**, 557–570 (2001).
69. Presley, J. F. *et al.* ER-to-Golgi transport visualized in living cells. *Nature* **389**, 81–85 (1997).
70. Nakata, T., Terada, S. & Hirokawa, N. Visualization of the dynamics of synaptic vesicle and plasma membrane proteins in living axons. *J. Cell Biol.* **140**, 659–674 (1998).
71. Stephens, D. J., Lin-Marq, N., Pagano, A., Pepperkok, R. & Paccaud, J. P. COPI-coated ER-to-Golgi transport complexes segregate from COPII in close proximity to ER exit sites. *J. Cell Sci.* **113**, 2177–2185 (2000).
72. Bonifacino, J. & Lippincott-Schwartz, J. Coat proteins: shaping membrane transport. *Nature Rev. Mol. Cell Biol.* **4**, 409–414 (2003).
73. Politz, J. C. Use of caged fluorophores to track macromolecular movement in living cells. *Trends Cell Biol.* **9**, 284–287 (1999).
74. Yokoe, H. & Meyer, T. Spatial dynamics of GFP-tagged proteins investigated by local fluorescence enhancement. *Nature Biotechnol.* **14**, 1252–1256 (1996).
75. Marchant, J. S., Stutzmann, G. E., Leissring, M. A., LaFeria, F. M. & Parker, I. Multiphoton-evoked color change of DsRed as an optical highlighter for cellular and subcellular labeling. *Nature Biotechnol.* **19**, 645–649 (2001).
76. Lukyanov, K. A. *et al.* Natural animal coloration can be determined by a nonfluorescent green fluorescent protein homolog. *J. Biol. Chem.* **275**, 25879–25882 (2000).
77. Elowitz, M. B., Surette, M. G., Wolf, P.-E., Stock, J. & Leibler, S. Photoactivation turns green fluorescent protein red. *Curr. Biol.* **7**, 809–812 (1997).
78. Sawin, K. E. & Nurse, P. Photoactivation of green fluorescent protein. *Curr. Biol.* **7**, R606–R607 (1997).
79. Patterson, G. H. & Lippincott-Schwartz, J. A photoactivatable GFP for selective photolabeling of proteins and cells. *Science* **297**, 1873–1877 (2002).
80. Ando, R., Hama, H., Yamamoto-Hino, M., Mizuno, H. & Miyawaki, A. An optical marker based on the UV-induced green-to-red photoconversion of a fluorescent protein. *Proc. Natl Acad. Sci. USA* **99**, 12651–12656 (2002).
81. Chudakov, D. M. *et al.* Kindling fluorescent proteins for precise *in vivo* photolabeling. *Nature Biotechnol.* **21**, 191–194 (2003).
82. Campbell, R. E. *et al.* A monomeric red fluorescent protein. *Proc. Natl Acad. Sci. USA* **99**, 7877–7882 (2002).
83. Zacharias, D. A., Violin, J. D., Newton, A. C. & Tsien, R. Partitioning of lipid-modified monomeric GFPs into membrane microdomains of live cells. *Science* **296**, 913–916 (2002).

84. Denk, W., Piston, D. W. & Webb, W. W. in *Handbook of Biological Confocal Microscopy* (ed. Pawley, J. B.) 445–458 (Plenum Press, New York, 1995).
85. Steyer, J. A. & Almers, W. A real-time view of life within 100 nm of the plasma membrane. *Nature Rev. Mol. Cell Biol.* **2**, 268–275 (2001).
86. Levin, M. H., Haggie, P. M., Vetrivel, L. & Verkman, A. S. Diffusion in the endoplasmic reticulum of an aquaporin-2 mutant causing human nephrogenic diabetes insipidus. *J. Biol. Chem.* **276**, 21331–21336 (2001).
87. Lippincott-Schwartz, J. *et al.* in *Green Fluorescent Proteins* (eds Sullivan, K. F. & Kay, S. A.) 261–281 (Academic Press, San Diego, 1999).

### Online links

#### DATABASES

The following terms in this article are linked online to:

**LocusLink:** <http://www.ncbi.nlm.nih.gov/LocusLink/>  
Arf1 | HMG17 | lamin-B receptor | MAPK | Sar1 | Sec13 | Sec23 | Sec24 | SF2 | TBP

**Protein Data Bank:** <http://www.rcsb.org/pdb/>  
DsRed | GFP | YFP

**Saccharomyces Genome Database:**  
<http://www.yeastgenome.org/>  
Fus3 | Ste5

Access to this interactive links box is free online.

#### REVIEW

## 4D imaging to assay complex dynamics in live specimens

Daniel Gerlich and Jan Ellenberg

A full understanding of cellular dynamics is often difficult to obtain from time-lapse microscopy of single optical sections. New microscopes and image-processing software are now making it possible to rapidly record three-dimensional images over time. This four-dimensional imaging allows precise quantitative analysis and enhances visual exploration of data by allowing cellular structures to be interactively displayed from many angles. It has become a key tool for understanding the complex organization of biological processes in live specimens.

Following the advent of indirect immunofluorescence during the 1960s, fluorescence microscopy has become an indispensable tool for localizing proteins in fixed specimens, and it often complements *in vitro* analyses of molecular mechanisms. The recent availability of a wealth of new vital markers for fluorescence microscopy<sup>1</sup> also allows defined molecular species to be conveniently labelled and, therefore, molecular assays to be carried out in live cells. In particular, green fluorescent protein (GFP) can be used to visualize virtually any protein in live cells<sup>2</sup>, and a large number of GFP variants are now available, which have different spectral properties<sup>3</sup> and allow simultaneous detection of multiple tagged proteins<sup>4</sup> (see also the review on page S1 of this supplement).

When highly dynamic and spatially complex structures, such as live cells and organisms, are imaged, a more complete representation is achieved by recording the data in three spatial dimensions over time (four-dimensional (4D) imaging)<sup>5–10</sup>. This generates complex data, typically consisting of thousands of individual image slices, which can occupy several gigabytes of storage space per experiment.

Such data require dedicated computational tools for their quantitative analysis. Here, we review typical 4D acquisition systems, important considerations for 4D experiments, and image-processing procedures for visualization and quantitation; in addition, we highlight the applications of this emerging approach in cell biology.

#### Acquiring 4D sequences

**General considerations for 4D imaging.** The fundamental consideration for any 4D live-cell imaging device is to keep the specimen alive during the acquisition of 100–10,000 images over a long period. A suitable and stable environment has to be provided, ensuring a constant temperature and a stably buffered culture medium. After this, the other significant concern in 4D imaging is the limited number of photons available to acquire fluorescence images from each cell. This is due to the limited number of fluorescent molecules that can be introduced into a cell at physiological concentrations and the limited photon yield before oxidation — which terminates fluorescence — for each fluorophore. Excessive illumination will lead to loss of

signal by photobleaching and is toxic for cells (see PHOTOTOXICITY). Therefore, excitation light is typically kept to a minimum in 4D experiments, which frequently results in a suboptimal signal-to-noise ratio and a lower spatial resolution when compared with images of fixed specimens. So, for each biological application, it is crucial to find a suitable compromise between sufficient, but not toxic, illumination, spatial resolution in the x, y and z axes, temporal resolution and the signal-to-noise ratio, so that the maximum number of acceptable images can be acquired before the specimen is completely photobleached or damaged. In some cases, a single z slice (2D time-lapse recording) can yield the best results — for example, when the structure of interest is flat and when there are no marked deformations along the z axis during the experiment. In this case, the lower number of frames in 2D time-lapse imaging would yield a better signal-to-noise ratio and a better time resolution, making it favourable to 4D imaging. Furthermore, when imaging dynamic processes in 4D, each of these parameters might change during the experiment and should be adjusted interactively.

A good illustration of this is 4D imaging of chromosome dynamics in mitotic cells (FIG. 1). For such an experiment, the time lapse would need to be shortened during more dynamic phases, such as congression — the rapid movement of chromosomes to the spindle equator in prometaphase — and then prolonged during the stable metaphase orientation. The number of z slices necessary is low in prophase, when the cell is still flatly attached to the substrate, and is increased when it rounds up in metaphase (see the side view in FIG. 1d,e). In addition, 4D experiments often run for hours or days to record a biological process such as one cell cycle. Therefore, automatic 4D recording with application protocols on 4D microscopes that can autofocus, track cell movements and revisit multiple-stage locations to follow several cells in parallel can markedly increase throughput and reproducibility of 4D imaging.

**Fluorescence microscopes for 4D imaging.** The main difference to conventional epifluorescence microscopy is that 4D imaging requires rapid and reproducible sectioning along the optical axis (z axis). Ideally, the acquisition time for each z stack should be small compared with the time lapse between the acquisition of individual stacks to avoid movements within each 3D data set. In addition, the z positions have to be highly reproducible over time, through many stacks, to avoid drifts. Z stepping (the movement